10th International Conference on Fracture Mechanics of Concrete and Concrete Structures
FraMCoS-X
G. Pijaudier-Cabot, P. Grassl and C. La Borderie (Eds)
https://doi.org/10.21012/FC10.235038

THE CONTRIBUTION OF STEEL FIBERS TO INCREASE THE DUCTILITY AND SERVICE LIFE IN RC BEAMS AND SLABS

THOMAZ E. T. BUTTIGNOL†, TÚLIO N. BITTENCOURT*, JULIANA F. FERNANDES†† AND JOSÉ L. A. O. SOUSA†††

† University of São Paulo (USP), São Paulo, SP Brazil
Av. Prof. Almeida Prado, trav.2, 271 Cidade Universitária, São Paulo, São Paulo/SP
e-mail: thomaz@usp.br

* University of São Paulo (USP), São Paulo, SP Brazil
Av. Prof. Almeida Prado, trav.2, 271 Cidade Universitária, São Paulo, São Paulo/SP
e-mail: tbitten@usp.br

†† University of São Paulo (USP), São Paulo, SP Brazil
Av. Prof. Almeida Prado, trav.2, 271 Cidade Universitária, São Paulo, São Paulo/SP
e-mail: julianaffernandes@gmail.com

††† University of Campinas, Campinas-SP, Brazil
Rua Saturnino de Brito, 224 Cidade Universitária Zeferino Vaz, Campinas - São Paulo
e-mail: jls.fec@gmail.com

Key words: Cyclic behavior, fiber reinforced concrete, toughness, damage model.

Abstract: Numerical and experimental analyses of RC beams and slabs reinforced with steel fibers and subjected to cyclic (4 Hz) four-point bending tests are carried out. The objective is to investigate the contribution of fibers to deflection control and increase of structural service life in elements with different inertia and height to length ratio. Fatigue causes a progressive damage in concrete structures due to microcracking diffusion and crack propagation, reducing the potential energy of the system, leading to increasingly ductility (larger deformations) and lower load carrying capacity. Experimental tests performed in the Hall of Technology at the Polytechnic School of the University of São Paulo demonstrated a reduction of vertical displacements of RC slabs reinforced with steel fibers (20 kg/m^3 and 60 kg/m^3). In contrast, RC beams reinforced with 20 kg/m^3 of steel fibers did not show any improvement in ductility. The results can be attributed, among others, to the higher toughness of RC slabs observed in monotonic loading tests and the statistical data dispersion of plain and fiber reinforced concrete beams in terms of S-N curves, as demonstrated in [1]. In order to better understand the differences between the RC beams and slabs reinforced with steel fibers, numerical analyses were carried out in the commercial software Abaqus 3D aiming to analyze crack propagation and stress distribution during cyclic loading. Crack propagation leads to a transfer of concrete tensile stresses to the reinforced bars and steel fibers, as demonstrated in [2]. Failure will occur due to the loss of equilibrium (critical crack length) and depletion (overall energy dissipation). The numerical models were calibrated with static tests. The results of the cyclic models demonstrated the importance to correctly take into account the size effect (strain localization both in compression and tension). A cross sectional multi-layer analysis is performed to analyze the current design procedures techniques. A closed form damage approach based on [3] is incorporated in the analysis. The results demonstrated the reliability of the multi-section approach to predict the deflections of RC beams and slabs, providing important information for design purposes and fatigue investigation.

1 INTRODUCTION

The continuous variation of the load in concrete structures can lead to fail due to fatigue as a result of the progressive damage of the material. The microcracking propagation and fracture cracks increase the dissipated energy, leading to a softening behavior and stress redistributions, reducing the modulus of elasticity and concrete stiffness as the effective section is reduced due to the flaws. The steel fibers, randomly distributed in the bulk concrete, are responsible to increase the material toughness and to control crack opening due to fibers bridging (pull out mechanism), leading to a more stable crack propagation. The incorporation of fibers in the concrete mix is important to guarantee a better response of the structure under cyclic and seismic loads. The energy absorption capacity (toughness) and the ductile behavior of FRC structures can prevent an abrupt failure by guaranteeing large deformations and internal stress redistributions (multicracking pattern). Fibers bridging are able to reduce damage, improving the structural durability. This is particularly important in the case of bridge deck and girders.

Cyclic tests performed by [4] on FRC beams submitted to 4PB tests and a step-by-step displacement-controlled loading and reloading up to failure, have demonstrated that both the cyclic flexural behavior and ductility are improved by fibers addition. However, the quantification of the material improvement due to fibers incorporation is still a challenge. The literature clearly demonstrates the superior properties of FRC materials, however, in some cases, this could be misleading. The incorporation of fibers increases the complexity of fatigue analysis. A comparison of experimental tests in literature carried out by [5] has shown a high scattering of the results from specimens with the same fiber content tested in bending. Moreover, in the case investigated, no benefit of steel fibers incorporation was noticed in RC beams reinforced with 20 kg/m^3 of steel fibers (F20) and subjected to four-point bending (4PB) cyclic loading. In contrast, RC slabs reinforced with steel fibers have demonstrated lower deflections directly proportional to the fibers amount (20 kg/m^3 and 60 kg/m^3).

One of the most important aspects concerning FRC design procedures is the role of the size effect. In tension, a fictitious crack model is usually adopted to describe concrete softening behavior in the post-peak regime. As a result, FRC analysis requires the introduction of the structural characteristic length [6-8] to describe the relationship between strain and crack opening. The characteristic length is correlated with the crack spacing, forcing the localization of the tensile stress softening model (post-peak constitutive equation). Numerical models have to take into account the characteristic length to avoid an overestimation of the energy dissipation of the crack band (fracture region idealized as a band of microcracks with constant width), since fibers contribute to sustain the fracture energy in higher levels compared to plain concrete [9].

Besides, slender members, such as slabs, are affected by compressive strain localization (plastic hinge mechanism) which induces higher deformations and rotations of the slabs [10-11]. The plastic hinge is developed due to the localization of plastic strains, caused by concrete damage in the compressive zone, occurring after the achievement of the maximum compressive stress. In the case of fatigue, a plastic hinge could be developed due to concrete non-linear and brittle behavior (hypoelasticity) which favors microcracking (damage zone) that tends to concentrate and localize the strains over a length of the compressive chord with a constant strain value. It is interesting noting that 4PB cyclic tests carried out in RC slabs have demonstrated higher deflections in relation to RC beams. This effect was not observed in Abaqus numerical analyses, suggesting the development of strain localization in the compressive zone, leading to higher

deformations. The slabs presented more distributed and closely spaced cracks in relation to the beams.

Said that, this paper discuss the role of the size effect in RC beams and slabs in the context of an investigation of the positive contribution of steel fibers to reduce midspan deflections and, as a result, increase the structural service life. Numerical analyses were carried out in the commercial software Abaqus 3D. Damage variables, obtained from an energy approach method [12] and the constitutive models from fib Model Code 2010 (MC 2010) [13], are incorporated in the analyses. The results are compared with experimental tests under 4PB quasi-static and cyclic loading. The variation of the vertical displacements and damage pattern in compression and tension are investigated. A cross-sectional analysis is also performed in order to analyze current design procedures techniques.

2 DAMAGE MODELS

Damage parameters in compression (d_c) and tension (d_t) were obtained as follows:

$$g_c = \int_{\varepsilon_{c0}}^{\varepsilon_{cu}} \sigma_c \cdot d\varepsilon_c$$

$$d_c = \frac{1}{g_c}\int_{\varepsilon_{c0}}^{\varepsilon_c} \sigma_c \cdot d\varepsilon_c \qquad (1)$$

$$g_t = \int_{\varepsilon_0^{cr}}^{\varepsilon_u^{cr}} \sigma_t \cdot d\varepsilon^{cr}$$

$$d_t = \frac{1}{g_t}\int_{\varepsilon_0^{cr}}^{\varepsilon^{cr}} \sigma_t \cdot d\varepsilon^{cr} \qquad (2)$$

where: g_c = compressive plastic energy per unit volume (area under the compressive parabolic stress-strain curve); g_t = tensile plastic energy per unit volume (area under the post-cracking tensile curve); σ_c = compressive stress; σ_t = tensile stress; ε_c = compressive strain; ε_{cr} = tensile crack strain.

The closed-form tensile damage equations for plain concrete (PC) and FRC were obtained as follows:

$$d_{t,pc} = 2 \cdot \frac{\varepsilon^{cr}}{\varepsilon_u^{cr}} \cdot \left(1 - \frac{\varepsilon^{cr}}{2 \cdot \varepsilon_u^{cr}}\right)$$

$$d_{t,frc} = \frac{f_{t0} \cdot \left(\varepsilon^{cr\,2}/2 - \varepsilon_u^{cr} \cdot \varepsilon^{cr}\right) - f_{FTU} \cdot \varepsilon^{cr\,2}/2 \cdot}{\varepsilon_u^{cr}} \cdot \frac{2}{f_{t0} \cdot \varepsilon_u^{cr}} \qquad (3)$$

The compressive damage parameters were calculated from the integration of the quadratic equation described in MC 2010, as shown in Figure 1. An initial linear-elastic branch is adopted and a tail in the compressive stress-strain curve is included in order to describe concrete residual softening behavior, which is determined from compressive tests performed with displacement control.

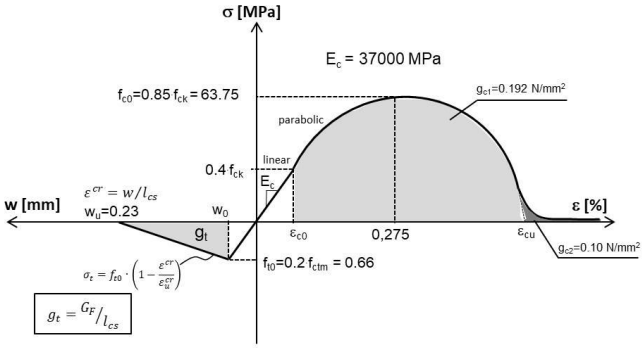

Figure 1: Plain concrete constitutive law.

In this case, only a numerical solution for the quadratic equation is possible and the definite integral is computed including upper and lower bound limits. In this case, the compressive plastic energy (g_c) is equal to 0.2 N/mm^2.

The characteristic length is introduced in the tensile constitutive law to describe the post-peak behavior (fictitious crack model), correlating the strain with the crack opening assuming $\varepsilon = w/l_{cs}$.

FRC classification and characterization was carried out in [14] following MC 2010 procedures. A linear post-peak stress-crack opening (ε-w) law was adopted, as shown in Table 1.

Table 1: FRC constitutive law: a) F20; b) F60

Class: 1b		Class: 5a	
σ_N (MPa)	w (mm)	σ_N (MPa)	w (mm)
0,5	0,05	2,25	0,0
0,15	2,5	0,25	2,5

The post-peak constitutive law in tension for PC and FRC are shown in Figure 2.

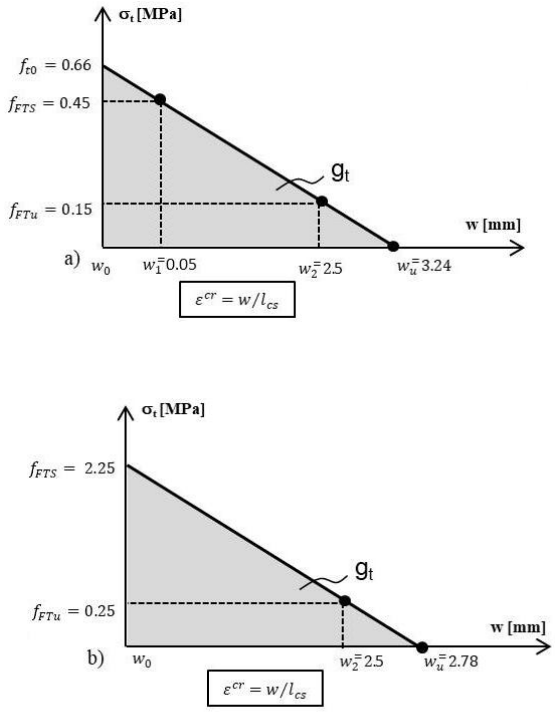

Figure 2: FRC post-peak constitutive law in tension: a) F20; b) F60.

3 NUMERICAL INVESTIGATION

Concrete was modeled assuming Abaqus "Concrete Damaged Plasticity" with the parameters described in Table 2.

Table 2: Concrete damaged plasticity parameters

Dilation	Eccentricity	f_{b0}/f_{c0}	K	Viscosity
38º	0.1	1,16	0.67	10^{-3}

The mechanical properties of the steel bars are shown in Table 3.

Table 3: Steel mechanical properties

Maximum stress (MPa)	500
Yielding stress (MPa)	500
Maximum elongation (%)	1,0
Modulus of Elasticity (MPa)	210.000

For Abaqus implementation, the strains were related to the crack opening assuming $\varepsilon = w/l_{cs}$. The values of the mesh size and characteristic length are shown in Table 4.

Table 4: Mesh size and characteristic length

	Beams	Slabs
Mesh size	30	60
Characteristic length	45	20

The values of l_{cs} were calibrated to avoid spurious energy and an underestimation of the flexural capacity. In the case investigated, the slabs exhibited higher values of toughness in relation to the beams (Figures 3 and 4) and closely spaced cracks. As a result, the post-cracking behavior, related to the crack spacing and crack width, is not the same due to the slabs lower dissipation of energy during crack propagation compared to the beams. Thus, for the same mesh size and the same material, one can expect lower values of the characteristic length for the slabs compared to the beams.

Damage was limited to a maximum value of 0.99 to avoid problems of lack of convergence during Abaqus processing. The stiffness recovery in compression and tension were defined according to Abaqus standard values (1.0 for tension to compression and 0 for compression to tension).

A comparison between the numerical and experimental values is carried out for beams and slabs, as shown respectively in Figures 3 and 4. The results demonstrate a good approximation of the numerical models with the experimental tests, except for the RC slab reinforced with 60kg/m^3 of fibers (Figure 4c), which has shown higher stiffness prior to steel bars yielding.

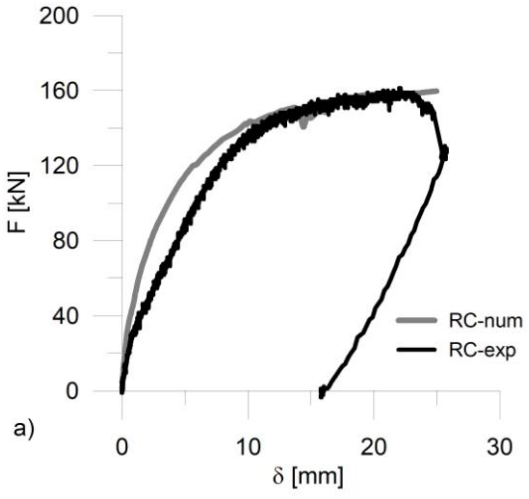

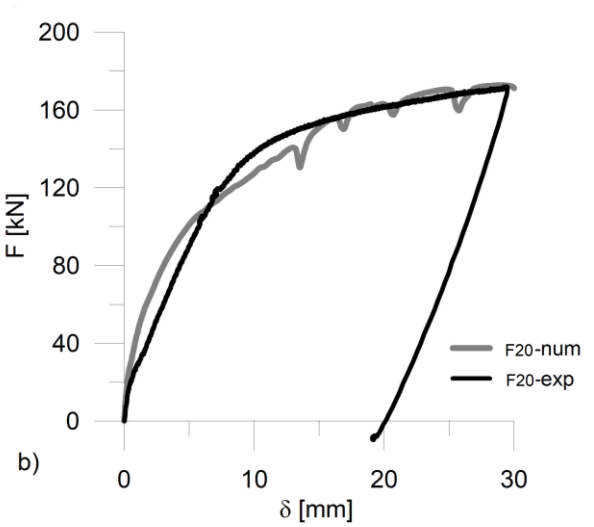

Figure 3: Comparison between experimental and numerical results of RC beams: a) RC; b) F20.

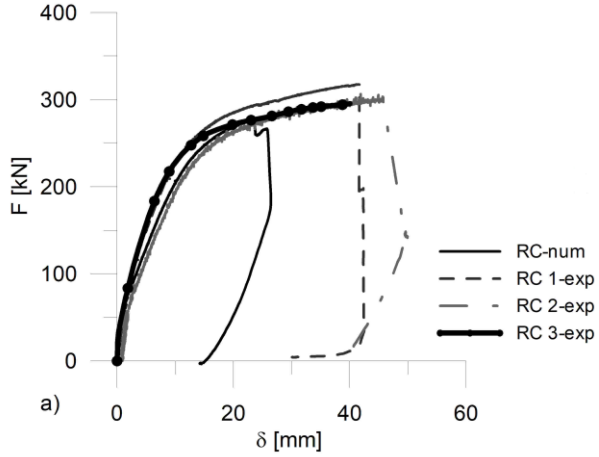

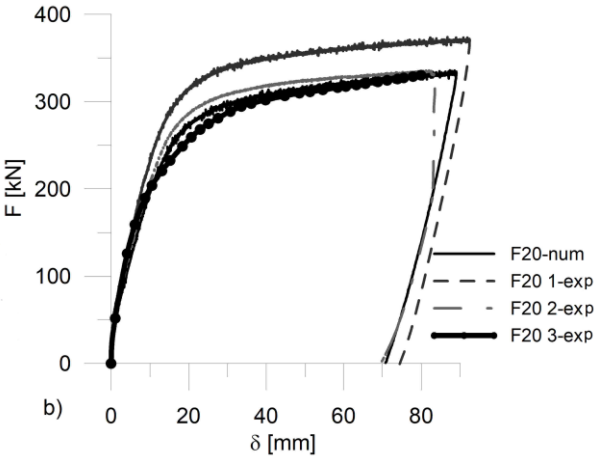

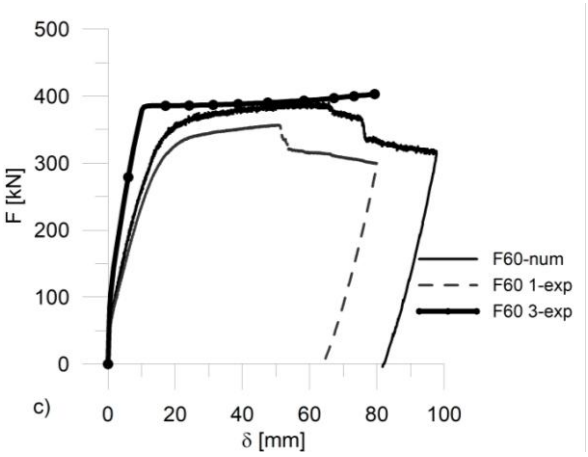

Figure 4: Comparison between experimental and numerical results of RC slabs: a) RC; b) F20; c) F60.

The tests demonstrate that the fibers contributed positively to increase the ductility and toughness of RC beams and slabs. In this case, the fibers were more effective in the slabs to reduce the energy dissipation and stabilize the crack propagation.

Cyclic tests were performed adopting a sinusoidal waveform with 4 Hz. The amplitude of the load level is shown in Table 5.

Table 5: Load levels for the cyclic tests.

	Minimum load level (kN)	Load variation (kN)	Maximum load level (kN)
Slabs	50	40	90
Beams	10	40	50

The experimental and numerical results of the cyclic analyses for beams and slabs are shown respectively in Figures 5 and 6. The RC slabs reinforced with fibers have shown higher stiffness and lower deformations. In contrast, no benefit of fibers incorporation was noticed for the RC beams.

The numerical results show a better approximation with the experimental tests for the RC beams. The RC slabs with no fibers and with 20 kg/m^3 of steel fibers presented deflection values approximately half of the experimental ones. The slab reinforced with 60 kg/m^3 of fibers demonstrated considerably lower vertical displacements.

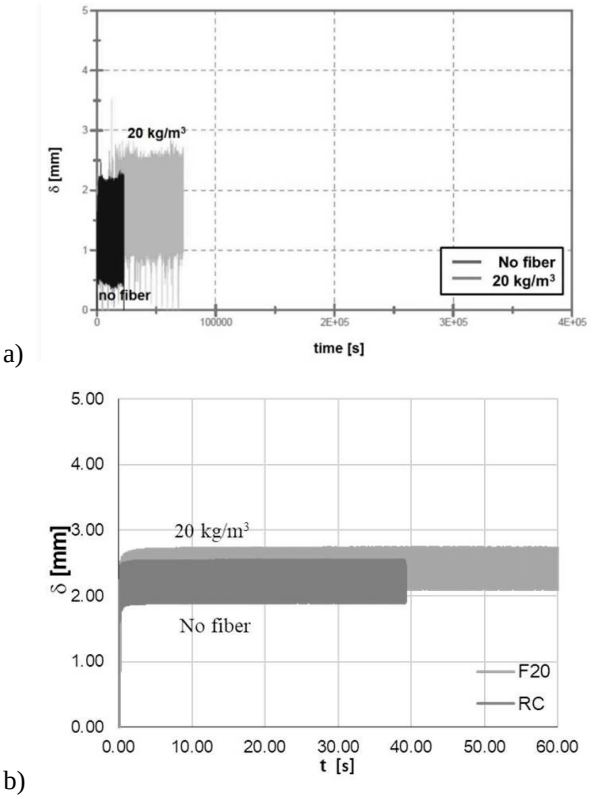

Figure 5: Cyclic numerical tests from RC beams: a) experimental; b) numerical.

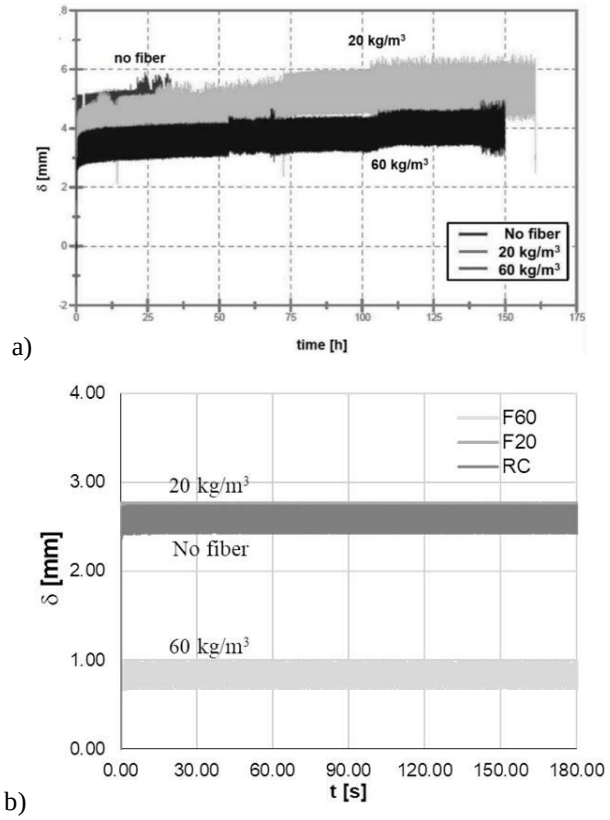

Figure 6: Cyclic numerical tests from RC slabs: a) experimental; b) numerical.

The differences between the behavior of beams and slabs can be attributed to the size effect and strain localization developed in the concrete compressive fiber, which leads to increased deformations and rotations of the slabs. Thus, numerical modeling should include the size effect of both the compressive and tensile fibers to obtain a better approximation, especially in the case of RC slabs with and without fibers addition.

The analysis of the compression damage of RC beams and slabs is shown in Figure 7. The results highlight the formation of the compressive struts in the beams. A more pronounced damaged area was developed in the RC beams, evidencing the positive effect of the fibers.

The tension damage is shown in Figure 8. The slabs show a more diffused damage, distributed over the bottom surface compared to the beams, where two major inclined cracks are developed over the cross-section, along the struts.

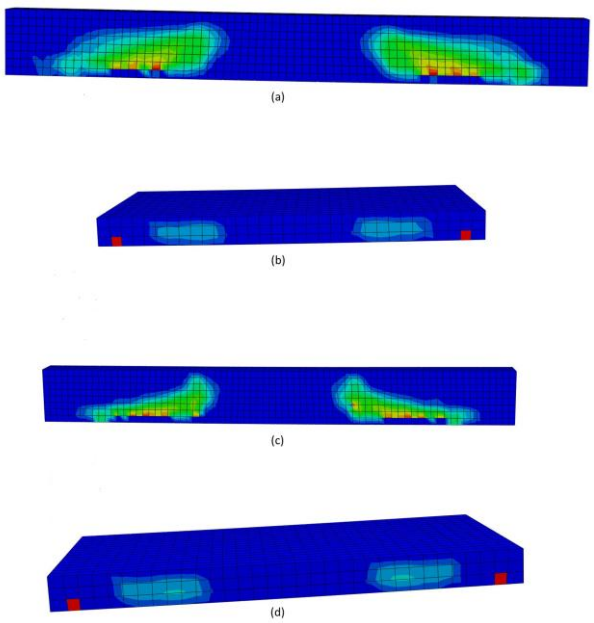

Figure 7: Damage in compression: a) RC beam; b) RC slab; c) Beam F20; d) slab F20.

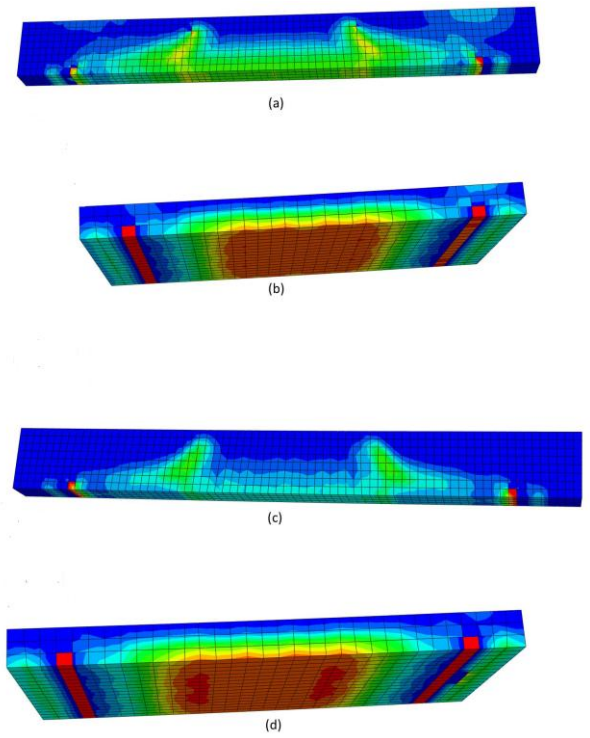

Figure 8: Damage in tension a) RC beam; b) RC slab; c) Beam F20; d) slab F20.

In order to investigate the size effect in compression (strain localization), a constitutive law including the characteristic length is adopted in compression, as described in [12]. The size effect can be described in terms of the plasticity theory, associating the strain localization and strength decay to the decrease of the material cohesion. The stress-strain relation in compression [12] is described as follows:

$$\sigma = f_c \cdot [(1+a)\cdot \exp(-b\cdot \varepsilon^p) - a\cdot \exp(-2\cdot b\cdot \varepsilon^p)]$$

$$a = 2\cdot \left(f_c/f_0\right) - 1 + 2\cdot \sqrt{\left(f_c/f_0\right)^2 - \left(f_c/f_0\right)}$$

$$b = f_0 \cdot \frac{l_{cs}}{G_{ch}} \cdot \left(1 + \frac{a}{2}\right) \qquad (4)$$

$$G_{ch} = \left(\frac{f_c}{f_{ct}}\right)^2 \cdot G_F$$

The numerical results for the RC slabs without fibers and with 20 kg/m^3 of fibers, assuming l_{cs} = 20 mm, are shown in Figure 9.

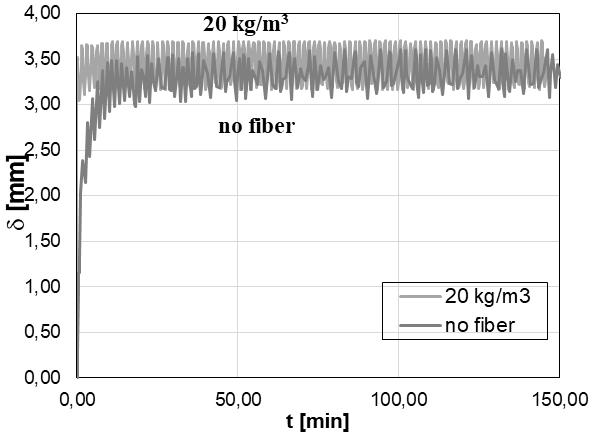

Figure 9: Cyclic numerical results for RC slabs.

The comparison between the two different numerical results (Figures 6b and 9) demonstrate that the introduction of the characteristic length in compression leads to a higher rotational capacity of the slabs and gives a better approximation with the experimental data (Figure 6a).

It is important to mention that the cyclic numerical analyzes demand an enormous computational cost and big storage data, which has limited the spectrum of the analysis to a small part of the experimental tests. More analyses are being developed in order to better understand the behavior of slabs under cyclic loading and to obtain a better approximation with the experimental results.

A cross-sectional analysis was also performed to investigate the current design procedures techniques.

4 CROSS-SECTIONAL ANALYSIS

A multilayer cross-sectional analysis was carried out in RC beams and slabs assuming a sinusoidal cyclic load (Table 5). The convergence was obtained with the equilibrium of both internal and external forces and moments.

The same residual constitutive laws utilized in the numerical analyzes (Figures 1 and 2) were implemented in the model.

The deflections were calculated adopting the effective Moment of Inertia assuming a cracked section and a weighted function (EI) to take into account concrete cracked and

uncracked sections. Damage variables were introduced to represent the stiffness degradation of the elements: $E_c = (1 - D) E_{c0}$. The equations are described below.

$$\delta = \frac{23}{648} \cdot \frac{P \cdot L^3}{EI}$$

$$EI = E_{sec} \cdot \left(I_2 \cdot \frac{L_1}{L} + I_c \cdot \frac{L_2}{L} \right)$$

$$I_2 = \frac{B \cdot x_2^3}{12} + \left(\frac{E_s}{E_c} - 1 \right) \cdot A_s \cdot (d - x_2)^2 \quad (4)$$

where: δ = vertical displacement; P = load; L = span; L_1 = uncracked length; L_2 = cracked length; E_{sec}= Secant Modulus of Elasticity ; EI = weighted flexural stiffness; M = bending moment; I_c = gross Moment of Inertia; I_2 = Moment of Inertia of cracked section at midspan.

The results for beams and slabs, in terms of deflections vs. time are shown respectively in Figures 9 and 10.

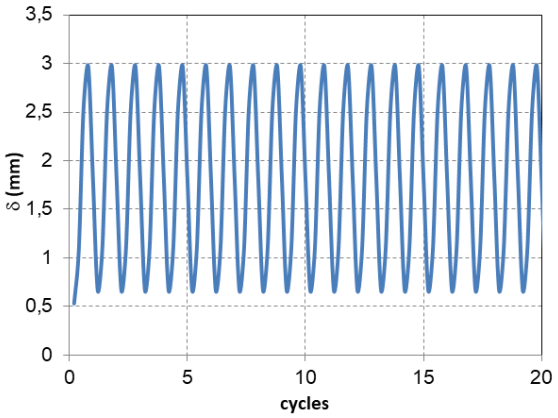

Figure 9: Deflections of RC beam.

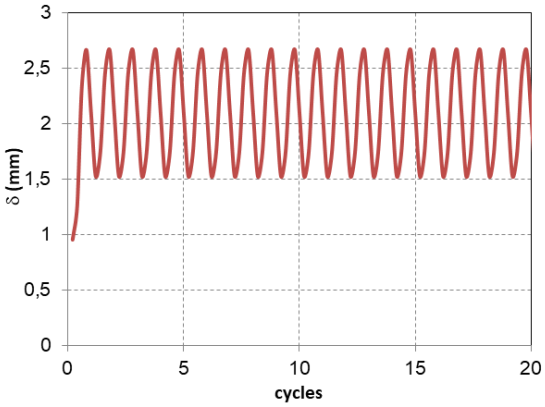

Figure 10: Deflections of RC slab.

The results demonstrate that the design procedures recommended for flexural static loading can be adopted for the cyclic analysis. In the case of RC slabs, due to the progressive damage and the member slenderness, the size effect (strain localization in the compressive zone) has to be taken into account. Assuming l_{cs} = 20 mm in Eq. 4, the deflections of the RC slab are determined as shown in Figure 11.

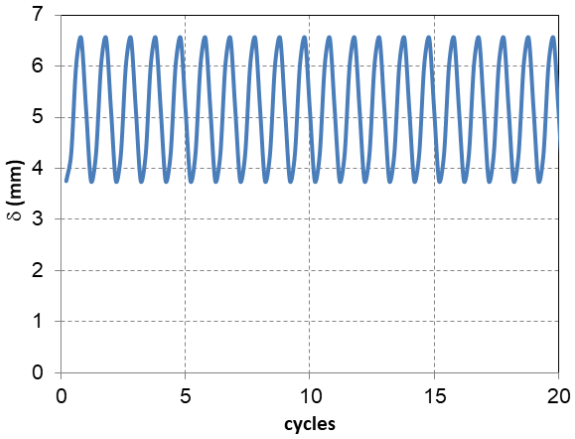

Figure 11: Deflections of RC slab (l_{cs} = 20 mm).

The result is closer to the experimental data, indicating that the strain localization in compression should be taken into account to correctly represent the structural behavior.

5 CONCLUSIONS

The results of the monotonic tests demonstrated that the fibers contributed positively to increase the ductility and toughness of RC beams and slabs. The fibers were more effective in the slabs to reduce the energy dissipation and stabilize the crack propagation, leading to closely spaced cracks. The numerical results show a good approximation with the experimental data. In this case, the correct definition of the characteristic length is important to avoid spurious energy during the analysis.

The RC slabs reinforced with fibers and submitted to 4PB cyclic loading have shown higher stiffness and lower deformations. In contrast, no benefit of fibers incorporation was noticed in the RC beams.

The cyclic numerical analyzes have shown a good correlation with the test data for the RC beams. In the case of RC slabs, the numerical

analyses underestimate the deflections due to the size effect (strain localization in the compressive chord). According to [15], concrete compressive softening behavior and strain localization can be described in terms of stress-deformation instead of stress-strain relationship, assuming a stress-strain relation that is strongly dependent of the depth of the compressive chord. A numerical analysis including the characteristic length also for the stress-strain in compression [12] was carried out. The results demonstrated a better approximation with the experimental data. The introduction of the characteristic length in compression has led to a higher rotational capacity of the slabs.

The cross-sectional analysis demonstrated that the design procedures for RC beams and slabs subjected to flexural quasi-static loading are also valid for cyclic loading and can be adopted to have a straightforward preliminary analysis of the structural behavior (deflections and stability). In the case of RC slabs, the strain localization in compression should be taken into account to correctly represent the structural behavior.

REFERENCES

[1] Lee, M. K, Barr, B. I. G, 2004. *An overview of the fatigue behaviour of plain and fibre reinforced concrete*. *Cement and Concrete Composites* v. 26 pp. 299–305.

[2] Parvez, A. and Foster, J. S., 2015. *Fatigue Behavior of Steel-Fiber-Reinforced Concrete Beams. Journal of Structural Engineering*, v. 141. Issue 4.

[3] Alfarah, B., López-Almansa, F. and Oller, S., 2017. *New methodology for calculating damage variables evolution in Plastic Damage Model for RC structures*. *Engineering Structures*; v. 132, pp. 70-86.

[4] Boulekbache, B., Hamrat, M., Chemrouk, M. and Amziane, S., *Flexural behaviour of steel fibre-reinforced concrete under cyclic loading. Construction and Building Materials* 126, (2016), pp. 253-262.

[5] Lee; M. K. and Barr, B. I. G. *An overview of the fatigue behaviour of plain and fibre reinforced concrete*. *Cement and Concrete Composites*, n. 26, pp. 299–305, 2004.

[6] Hillerborg, A.; Modeer, M. and Peterson, P. E. *Analysis of crack formation and crack growth by means of fracture mechanics and finite elements*. *Cement and Concrete Research*, no. 6, pp. 773-782, 1976.

[7] Bazant, Z. P.; Cedolin, L. *Stability of Structures: Elastic, Inelastic, Fracture and Damage Theories*. *Oxford University Press, New York, 2nd. edition*, 2003.

[8] Irwin, G. *Analysis of stresses and strains near the end of a crack traversing a plate*. J. Appl. Mech., v. 24, pp. 361–364, 1957.

[9] Di Prisco, M., Colombo, M. and Colombo, I. *The Role of the Structural Characteristic Length in FRC Structures*. *Proceedings of the 9th International Conference on Fracture Mechanics of Concrete and Concrete Structures - FraMCoS-9*, 2016.

[10] Walraven, J. C. *Fracture mechanics of concrete and its role in explaining structural Behaviour*. *Proceedings of the 6th International Conference on Fracture Mechanics of Concrete and Concrete Structures - FraMCoS-6*, 2007.

[11] Bigaj, A. and Walraven, J.C. Size Effects in Plastic Hinges of Reinforced Concrete Members. Delft University of Technology, Heron, V. 47, n. 2, pp. 79-80, 2002.

[12] Lubliner, J. et al. *A Plastic Damage Model for Concrete. Int. J. Solids Structures* Vol. 25, No.3, pp. 299--326, 1989.

[13] FIB – International Federation for Structural Concrete. *Fib Model Code for Concrete Structures 2010. Berlin: Verlag Ernst & Sohn*, 2013.

[14] Buttignol, T. E. T., et al. *Design of reinforced concrete beams with steel fibers in the ultimate limit state. Ibracon Structures and Materials Journal*, v. 11, n. 5, pp. 997 – 1024, 2018.

[15] Hillerborg, A. *Fracture mechanics concepts applied to moment capacity and rotational capacity of reinforced concrete beams. Engineering Fracture Mechanics*, V. 35, Issues 1-3, pp. 233–240, 1990.